Negative thermal expansion in nanostructured intermediate valence $YbAl_3$

C. Echevarria-Bonet[1*], M. de la Fuente Rodriguez[2], J. I. Espeso[2], J. A. Blanco[1], Inés Puente Orench[3,4], D. P. Rojas[5], L. Rodríguez Fernández[6], F. Fauth[7] and L. Fernández Barquín[2]

[1] *Department of Physics, University of Oviedo, 33007 Oviedo, Spain*
[2] *CITIMAC, Facultad de Ciencias, Universidad de Cantabria, 39005 Santander, Spain*
[3] *Institut Laue-Langevin, 71 Avenue des Martyrs, CS 20156, 38042 Grenoble Cedex 9, France*
[4] *Instituto de Ciencia de Materiales de Aragón, CSIC-Universidad de Zaragoza, 50009 Zaragoza, Spain*
[5] *Dpto. Estructuras y Física, ETSAM, Universidad Politécnica de Madrid, 28040 Madrid, Spain*
[6] *SERMET, Universidad de Cantabria, 39005 Santander, Spain*
[7] *CELLS - ALBA synchrotron, E-08290 Cerdanyola del Vallès, Barcelona, Spain*

Abstract—. Interest in strongly correlated electron system $YbAl_3$ has been recently renewed by the observation of a breakdown of coherence effects and Fermi liquid behavior when the alloy reduces its particle size down to around 11 nm. Powder diffraction measurements using neutron and synchrotron radiation allow us to estimate the thermal expansion of the nanostructured $YbAl_3$. There is a region of negative thermal expansion in the nanostructured material at higher temperatures compared to that of bulk $YbAl_3$. This result shows that reducing the size of $YbAl_3$ not only affects electronic properties, but also the lattice dynamics of this material.

Index Terms—. Intermediate valence, Nanomagnetics, thermal expansion, neutron diffraction, synchrotron XRD diffraction.

I. INTRODUCTION

The strongly correlated electron system (SCES) $YbAl_3$ alloy has attracted much attention in the last decades due to the fact that it exhibits a great variety of cutting-edge physical phenomena, such as intermediate valence (IV), Kondo resonance and Fermi-liquid (FL) behavior [van Daal 1974]. All these behaviors are related to the hybridization of the 4f-state with the conduction band electrons. Among the great variety of experiments performed in $YbAl_3$ we could cite magnetic [Hiess 2000] or thermoelectric [Rowe 2002] measurements and the effect of the hydrostatic pressure [Ohara 2010] or the magnetic field (and disorder) [Ebihara 2003], procuring a great deal of complementary information on the just related attractive phenomena. Valence fluctuations have been observed in both bulk [Suga 2005] and nanostructured alloys [Rojas 2008], leading to changes in the Fermi surface topology (Lifshiftz transition) of the Kondo lattice IV $YbAl_3$ [Chatterjee 2017].

In bulk form, this alloy crystallizes in the cubic $AuCu_3$-type structure (Pm-3m), with a cell parameter a=4.2036(3) Å [Moriarty 1966]. Temperature dependent magnetic susceptibility has been found to have a broad maximum at around 125 K and to follow a Curie-Weiss law with an effective moment 4.2 μ_B [Bauer 2004]. The well-known maximum in the magnetic susceptibility appears in IV compounds and is consistent with a high Kondo temperature T_K~600-700 K [Bud'ko 2008]. Below 40 K, a Fermi-liquid behavior (T^2 dependence of the electrical resistivity) is observed, connected to a coherence temperature of 40 K [Bauer 2004].

A change in the Kondo lattice behavior of bulk $YbAl_3$ has been observed when the alloy is in the nanoparticle state (≈12 nm). Measurements of the electrical resistivity show inhibited coherence effects and deviation from the standard Fermi liquid behavior (T^2-dependence). These results are interpreted as being due to the effect of the disruption of the periodicity of the array of Kondo ions provoked by the size reduction process [Echevarria-Bonet 2018]. Coherence effects, observed in bulk $YbAl_3$ [Bauer 2004], have been observed to be modified when nanostructuring this alloy [Echevarria-Bonet 2018]. In this sense, $Yb_{1-x}Lu_xAl_3$ series of bulk alloys have been also studied and changes in specific heat, susceptibility and electrical resistivity were found, suggesting that coherence effects are very sensitive to lattice order [Ebihara 2003].

Moreover, negative thermal expansion (NTE) has been observed in bulk $YbAl_3$ at low temperatures (T<20K), while for the diluted alloy, $Yb_{0.1}Lu_{0.9}Al_3$, this region of NTE is not present [Bud'ko 2008], relating the presence of an Yb intermediate valence state to the existence of NTE. This behavior, or that of an almost zero thermal expansion, is not restricted to intermediate valence systems only. The classic example is the well-known $Fe_{0.64}Ni_{0.36}$, Invar alloy [Guillaume 1897], but there are other simpler systems, such as Au [Li 2002] or CuO [Zheng 2008] which have been reported to present NTE as nanoparticles but not in bulk, in different temperatures ranges [Attfield 2018]. NTE has also been observed in systems such as the frustrated magnetic insulator $CdCr_2O_4$ [Rossi 2019], rare-earth intermetallic alloys R_2Fe_{17} (R=Rare Earth) [Alvarez-Alonso 2011] or the permanent magnet family $R_2Fe_{14}B$ [Buschow 1987].

II. EXPERIMENTAL TECHNIQUES

A starting polycrystalline $YbAl_3$ pellet was prepared by arc melting of suitable amounts of pure constituents Yb(3N), Al(5N) (Alfa) under protective Ar atmosphere. It was subsequently annealed at 750 °C for five days in vacuum (~10^{-3} mbar) in order to improve crystallinity and ensure homogenization of samples. The reduction in the particle size of bulk $YbAl_3$ was achieved by mechanical milling, which is considered a practical route to obtain large quantities of nanocrystalline materials. Amounts around 4 g of bulk $YbAl_3$ were crushed and then milled in a planetary high-energy ball milling system Retsch PM 400/2 at a rotation speed of 200 rpm. The initial powders were placed in tungsten carbide containers using a ball/sample weight ratio of 12:1. These containers were hermetically closed in a glove box in an Ar (99.99%) atmosphere to minimize powder oxidation. The milling procedure was carried out following successive steps of 5 min of clockwise and anti-clockwise rotation with a 5 min intermediate stop. Material was collected at 70 hours of milling time. In order to avoid oxidation, handling and storage were carried out in a glove box under argon atmosphere.

Synchrotron radiation powder x-ray diffraction (SR-PXD) patterns were acquired room temperature (RT) in the MSPD beamline at ALBA synchrotron (wavelength, λ = 0.4126 Å). Powder neutron diffraction (ND) experiments were carried out in the diffractometer D1B, ILL (France) using λ = 2.52 Å. A temperature dependent study was performed, from 2 to 300K.

XRD and ND patterns were refined by the Rietveld method (through the FULLPROF Suite [Rodriguez-Carvajal 1993]) including resolution function calibration standards, thus taking into account the instrumental broadening. The fit was carried out using a Thompson-Cox-Hastings function, allowing the calculation of the particle size (D) and strain (η).

Transmission electron microscopy (TEM) was performed in a Jeol 2100 microscope in order to check the nanocrystalline arrangement.

DC magnetization measurements were performed in a Quantum Design PPMS, in a standard zero field-cooled (ZFC) protocol, with μ_0H=1T in the temperature range 2–300 K.

III. RESULTS

A. Structural characterization

The analysis of the x-ray diffraction pattern of the bulk alloy is consistent with a cubic crystal structure of the $AuCu_3$-type (space-group Pm-3m) with a refined unit-cell parameter a=4.2023(1) Å, in good agreement with previously reported data [Palenzona 1972]. A small percentage of $YbAl_2$ is also found in the patterns. This fact has been observed previously [Görlach 2005] and subsequent mechanical milling results in helping reaction to finish and $YbAl_3$ is formed [Echevarria-Bonet 2014].

Fig. 1 shows the SR-PXD patterns of the 70h milled $YbAl_3$ alloy (hereinafter 70h-$YbAl_3$) at RT. Rietveld refinements provided the same structure than in the bulk (cubic, Pm-3m) with a lattice parameter a=4.2076(1) Å. Particle size was decreased down to D=11(1) nm and strain increased up to η=0.40(1)%. The refinements led to reliability factors χ^2=2.56 and R_B=5.42 (for the $YbAl_3$ phase). Traces of $YbAl_2$ were also found in the patterns, accounting less than 1 wt.%, as obtained after Rietveld refinements. These values are similar to those obtained in other $YbAl_3$ milled alloys [Echevarria-Bonet 2018] and in the same order of magnitude of those found by TEM results. Indeed, TEM, shown in the inset of Fig. 2, confirms the order of magnitude of the mean particle size.

B. Magnetic characterization

Figure 4 shows the temperature dependence of the magnetization for both bulk (data taken from literature [Rojas 2008]) and 70h-$YbAl_3$, for comparison. Two main features are visible: (i) a broad maximum whose center is slightly shifted to higher temperatures for the milled alloy (T_{max} = 125 K for bulk [Bauer 2004] while T_{max} = 133 K for 70h-$YbAl_3$) and (ii) a plateau of the magnetization curve at low temperatures (around 20K) followed by an upturn for T<20 K.

This broad maximum is usually associated with a Kondo behavior. A Kondo temperature T_K of the order of 600 K has been found for $YbAl_3$ bulk [Bud'ko 2008]. If we scale the T_{max} with this Kondo temperature for both bulk and milled alloy, an approximate value of T_K~650 K can be estimated for the 70h-$YbAl_3$ compound. In order to provide a more accurate value of T_K, quasielastic neutron scattering experiments should be performed. This result is in good agreement with the increase of the Debye temperature found in the thermal expansion behavior above, that also indicated a T_K enhancement, modifying the coherence effects at low temperatures, as it has also been observed in previous results of milled $YbAl_3$ alloys [Echevarria-Bonet 2018]. The behavior of the curves here is in good agreement with those in literature [Rojas 2008] for milled $YbAl_3$ alloys though T_{max} values are slightly different. Ohara *et al*. (2010) observed, in $YbAl_3$ single crystals, not only a subtle shift of the T_{max} to lower temperatures but also an enhancement of the magnetic susceptibility with increasing pressure (1.07GPa) [Ohara 2010]. Somehow, this could indicate a negative pressure-like effect when $YbAl_3$ is nanostructured. This same effect is observed in $Yb_{1-x}Lu_xAl_3$, in which the T_{max} shifted to higher temperatures with increasing Lu concentration [Bauer 2004], leading to the idea that nanostructuring this alloy is similar to applying negative pressure or chemical tuning. Not only the T_{max} shifts to higher temperatures but also the value of the magnetic susceptibility decreases with milling, as it does with higher Lu concentrations [Bauer 2004]. This decrease of the magnetic susceptibility is a significant sign of the increasing presence of Yb^{2+} contribution (non magnetic) at high temperatures [Rojas 2008]. If we take into account the Coqblin-Schriefer model, $\chi(0) \propto 1/T_K$ [Rajan 1983], the decrease of the magnitude of the magnetic susceptibility would lead to an increase of the Kondo temperature, consistently with thermal expansion results and the position of T_{max} in the magnetic susceptibility (see Fig. 4). This has also been observed in other Yb-based compounds, such as in the $Yb_{1-x}Y_xCuAl$ series [Rojas 2018].

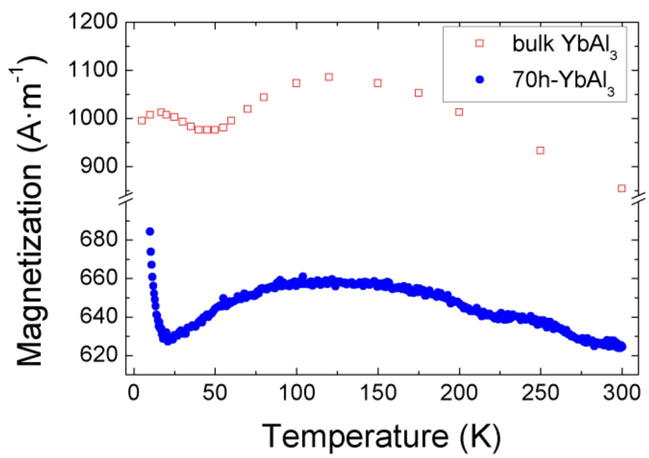

Figure 4. Temperature dependent magnetization curves for the bulk (data from [Rojas 2008]) and the 70h-$YbAl_3$ milled alloy. A non-negligible contribution of $YbAl_2$ is visible at around 250 K, as found in diffraction experiments.

Regarding (ii), the upturn of the magnetization (or susceptibility) at low temperatures may be related to the presence of magnetic impurities or to the change of degrees of freedom. The latter can be understood as a modification of the structure of the alloys when nanostructuring, leading to the increase of the Yb^{3+} contribution on the surface of the particles at low temperatures. Signs of valence change with temperatures have been observed in this analysis. It would be of interest to follow the valence fluctuations with temperatures for milled alloys.

IV. CONCLUSION

In conclusion, we have shown that the reduction of size (~11 nm) in strongly correlated electron system $YbAl_3$ has not only electronic effects in the Kondo temperature (from 600 K in bulk to approximately 650 K in nanostructured material) and changes in the coherence effects and in the low-temperature Fermi-liquid behavior, but also has important consequences in the lattice dynamics, because the region of the negative thermal expansion is slightly larger (below 40 K) when compared to that of the bulk (below 20 K). Magnetization results at low temperatures are intriguing and additional experiments are needed to further elucidate the origin of the upturn at low temperatures.

ACKNOWLEDGMENT

This work was supported by projects MAT2017-83631-C3-3-R (Spanish ‘Ministerio de Ciencia, Innovación y Universidades’) and GRUPINN IDI/2018/000185 (Principado de Asturias, Spain). C.E.-B. would like to thank funding from Banco Santander for their “Mobility grant for professors and researchers from University of Oviedo” (2019).

REFERENCES

Álvarez-Alonso P, Gorria P, Blanco J A, Sánchez-Marcos J, Cuello G J, Puente-Orench I, Rodríguez-Velamazán J A, Garbarino G, de Pedro I, Rodríguez Fernández J and Sánchez Llamazares J L (2011), “Magnetovolume and magnetocaloric effects in Er_2Fe_{17}”, *Phys. Rev. B*, vol. 86, p.184411.

Arvanitidis J, Papagelis K, Margadonna S, Prassides K and Fitch A N (2003), “Temperature-induced valence transition and associated lattice collapse in samarium fulleride”, *Nature*, vol. 425, pp. 599-602.

Attfield J P (2018), “Mechanisms and Materials for NTE”, *Front. Chem*. vol. 6, p. 371.

Bauer E D, Booth C H, Lawrence J M, Hundley M F, Sarrao J L, Thompson J D, Riseborough P S and Ebihara T (2004), “Anderson lattice behavior in $Yb_{1-x}Lu_xAl_3$”, *Phys. Rev. B*, vol. 69, p. 125102.

Bud’ko S L, Frederick J C, Mun E D, Canfield P C and Schmiedeshof G M (2008), “Thermal expansion, heat capacity and magnetostriction of RAl_3 (R = Tm, Yb, Lu) single crystals”, *J. Phys.: Condens. Matter*, vol.20, p.025220.

Buschow K H J and Grössinger R (1987), “Spontaneous volume magnetostriction in $R_2Fe_{14}B$ compounds”, J. Less-Common Met. vol. 135, p. 39.

Chatterjee S, Ruf J P, Wei H I, Finkelstein K D, Schlom D G and Shen K M (2017), “Lifshitz transition from valence fluctuations in $YbAl_3$”, Nature Communications, vol. 8, p.852.

Ebihara T, Bauer E D, Cornelius A L, Lawrence J M, Harrison N, Thompson J D, Sarrao J L, Hundley M F and Uji S (2003), “Dependence of the effective masses in $YbAl_3$ on magnetic field and disorder”, *Phys. Rev. Lett.*, vol. 90, p. 166404.

Echevarria-Bonet C (2014), “Size induced electronic and magnetic changes in nanometric rare earth alloys”, PhD thesis, Universidad de Cantabria.

Echevarria-Bonet C, Rojas D P, Espeso J I, Rodríguez Fernández J, Rodríguez Fernández L, Bauer E, Burdin S, Magalhães S G, Fernández Barquin L (2018), “Breakdown of the coherence effects and Fermi liquid behavior in $YbAl_3$ nanoparticles”, *Journal of Physics: Condensed Matter*, vol. 30, p.135604.

Gegenwart P (2016), “Grüneisen parameter studies on heavy fermion quantum criticality”, *Rep. Prog. Phys.*, vol 79, p. 114502.

Görlach T, Pfleiderer C, Grube K and Löhneysen H v (2005), “Low-temperature properties of $YbAl_2$”, *Phys. Rev. B*, vol. 71, p. 033101.

Guillaume C E (1897), “Recherches sur les aciers au nickel. dilatations aux temperatures elevees; resistance electrique”, *Comptes Rendus de l’Academie des Sciences*, vol. 125, pp. 235-238.

Hiess A, Boucherle J X, Givord F, Schweizer J, Lelièvre-Berna E, Tasset F, Gillon B and Canfield P C (2000), “Magnetism in intermediate-valence $YbAl_3$: a polarized neutron diffraction study”, *Journal of Physics: Condensed Matter*, vol. 12, p. 829.

Iandelli A and Palenzona A (1972), “Magnetic susceptibility and expansion coefficient of the intermetallic compounds $YbAl_2$ and $YbAl_3$”, *Journal of the Less Common Metals*, vol. 29, pp. 293-297.

Kumar R S, Svane A, Vaitheeswaran G, Kanchana V, Bauer E D, Hu M, Nicol M F and Cornelius A L (2008), “Pressure-induced valence change in $YbAl_3$: A combined high-pressure inelastic x-ray scattering and theoretical investigation”, *Phys. Rev. B*, vol. 78, p. 075117.

Li W H, Wu S Y, Yang C C, Lai S K, Lee K C, Huang H L, Yang H D (2002), “Thermal contraction of Au nanoparticles”, *Phys. Rev. Lett*. vol. 89, p. 135504.

Matsumoto Y, Kuga K, Tomita T, Küchler R and Nakatsuji S (2017), “Anisotropic Thermal Expansion of α-YbAlB4”, *Journal of Physics: Conf. Series,* vol. 807, p. 022005.

Moriarty J L Jr; Humphreys J E; Gordon R O; Baenziger N C (1966), “X-ray examination of some rare-earth-containing binary alloy systems”, *Acta Crystallographica*, vol. 21, pp. 840-841.

Ohara S, Adachi Y, Yamashita T and Sakamoto I (2010), “Pressure effects on magnetic susceptibility of intermediate-valence compound $YbAl_3$”, *Journal of Physics: Conference Series*, vol. 200, p. 012150.

Palenzona A (1972), “The ytterbium-aluminum system”, *J. Less-Common Met.*, vol. 29, pp. 289-292.

Rajan V T (1983), “Magnetic Susceptibility and Specific Heat of the Coqblin-Schrieffer Model”, *Phys. Rev. Lett*., vol. 51, p. 308.

Rodríguez-Carvajal J (1993), “Recent advances in magnetic structure determination by neutron powder diffraction”, *Physica B*, vol. 192, pp. 55-69.

Rojas D P, Fernández Barquín L, Espeso J I, Rodríguez Fernández J, Chaboy J (2008), “Reduction of the Yb valence in $YbAl_3$ nanoparticles”, Phys. Rev. B, vol. 78, p. 094412.

Rojas D P, Gandra D G, Medina A N, Fernández Barquín L, Gómez Sal J C (2018), “Kondo temperature and Heavy Fermion behavior in $Yb_{1-x}Y_xCuAl$ series of alloys”, *Physica B*, vol. 536, pp. 176-181.

Rossi L, Bobel A, Wiedmann S, Küchler R, Motome Y, Penc K, Shannon N, Ueda H and Bryant B (2019), “Negative Thermal Expansion in the Plateau State of a Magnetically Frustrated Spinel”, *Phys. Rev. Lett*., vol. 123, p. 027205.

Rowe D M, Kuznetsov V L, Kuznetsova L A and Min G (2002), “Electrical and thermal transport properties of intermediate valence $YbAl_3$”, *Journal of Physics D: Applied Physics*, vol. 35, p. 2183.

Sa B, Zhou J and Sun Z (2012), “First-principles investigation of mechanical and thermodynamic properties of the rare earth intermetallic $YbAl_3$ under pressure”, *Intermetallics*, vol. 22, pp. 92-98.

Sayetat F, Fertey P and Kessler M (1998), “An Easy Method for the Determination of Debye Temperature from Thermal Expansion Analyses”, J. Appl. Cryst., vol. 31, pp. 121-127.

Suga S, Sekiyama A, Imada S, Shigemoto A, Yamasaki A, Tsunekawa M, Dallera C, Braicovich L, Lee T L, Sakai O, Ebihara T and Ōnuki Y (2005), “Kondo Lattice Effects of $YbAl_3$ Suggested by Temperature Dependence of High-Accuracy High-Energy Photoelectron Spectroscopy”, *J. Phys. Soc. Jpn*. 74 2880.

Thacher A C J (1960), “Rational Approximations for the Debye Functions”, J. *Chem. Phys.* vol. 32, p. 638.

van Daal H J, van Aken P B and Buschow K H J (1974), “The seebeck coefficient of $YbAl_2$ and $YbAl_3$”, *Physics Letters A*, vol. 49, p. 246.

Yamada I, Shiro K, Etani H, Marukawa S, Hayashi N, Mizumaki M, Kusano Y, Ueda S, Abe H and Irifune T (2014), “Valence Transitions in Negative Thermal Expansion Material $SrCu_3Fe_4O_{12}$”, *Inorg. Chem*. vol. S3, pp. 10563-10569.

Zheng X G, Kubozono H, Yamada H, Kato K, Ishiwata Y and Xu C N (2008), “Giant negative thermal expansion in magnetic nanocrystals”, *Nature Nanotechnol*. vol. 3, pp. 724–726.